



LAWRENCE
LIVERMORE
NATIONAL
LABORATORY

Slow Strain Rate Testing of Alloy 22 in Simulated Concentrated Ground Waters

Kenneth J. King, Lana L. Wong, John C. Estill,
Raul B. Rebak

October 29, 2003

CORROSION/2004
New Orleans, LA, United States
March 28, 2004 through April 1, 2004

Disclaimer

This document was prepared as an account of work sponsored by an agency of the United States Government. Neither the United States Government nor the University of California nor any of their employees, makes any warranty, express or implied, or assumes any legal liability or responsibility for the accuracy, completeness, or usefulness of any information, apparatus, product, or process disclosed, or represents that its use would not infringe privately owned rights. Reference herein to any specific commercial product, process, or service by trade name, trademark, manufacturer, or otherwise, does not necessarily constitute or imply its endorsement, recommendation, or favoring by the United States Government or the University of California. The views and opinions of authors expressed herein do not necessarily state or reflect those of the United States Government or the University of California, and shall not be used for advertising or product endorsement purposes.

17October2003

Paper04548tobepresentedattheNACEInternational,CORROSION/04ConferenceinNewOrleans,
LA28Marchto01April2004

SLOW STRAIN RATE TESTING OF ALLOY 22 IN SIMULATED CONCENTRATED GROUNDWATERS

Kenneth J. King, Lana L. Wong, John C. Estill and Raúl B. Rebak

Lawrence Livermore National Laboratory, Livermore, CA, 94550

ABSTRACT

The proposed engineering barriers for the high-level nuclear waste repository in Yucca Mountain include a double-walled container and a detached drip shield. The candidate material for the external wall of the container is Alloy 22 (N06022). One of the anticipated degradation modes for the containers could be environmentally assisted cracking (EAC). The objective of the current research was to characterize the effect of applied potential and temperature on the susceptibility of Alloy 22 to EAC in simulated concentrated water (SCW) and other environments using the slow strain rate technique (SSRT). Results show that the temperature and applied potential have a strong influence on the susceptibility of Alloy 22 to suffer EAC in SCW solution. Limited results show that sodium fluoride solution is more detrimental than sodium chloride solution.

Keywords: nuclear waste container, N06022, environmentally assisted cracking (EAC), slow strain rate technique (SSRT), applied potential, simulated concentrated water (SCW), temperature

INTRODUCTION

The current design concept for the high-level nuclear waste containers in the USA is based on a metallic multi-barrier system. This design specifies an external layer of Alloy 22 (N06022) and an internal layer of type 316 stainless steel (S31603).¹⁻³ Alloy 22 is a nickel (Ni) based alloy that contains approximately 22% chromium (Cr), 13% molybdenum (Mo), 3% tungsten (W) and 3% iron (Fe).⁴ The main purpose of the internal barrier is to provide structural integrity and to contribute to the shielding of radiation. The main role of the external barrier is to provide protection against corrosion.^{1,3} Alloy 22 is widely used in industrial corrosive applications since it can tolerate a wider range of conditions, from reducing to oxidizing and from acidic to alkaline.⁵⁻⁹ In the presence of water, there are three main modes of corrosion that Alloy 22 may undergo at the emplacement site in Yucca Mountain, namely general corrosion, localized corrosion and environmentally assisted cracking (EAC).¹⁰ EAC may include degradation mechanisms such as stress corrosion cracking (SCC) and hydrogen induced cracking (HIC) or hydrogen embrittlement (HE).

Millannealed Alloy 22 is highly resistant to SCC in acidic concentrated chloride solutions.^{2,11-16} Dunn et al. did not find SCC when they tested Alloy 22 in 14 molal Cl^- (as MgCl_2) at 110°C and 9.1 molal LiCl at 95°C under controlled potential.^{11,13-14} They used wedge opening loaded double cantilever beam (DCB) and compact tension (CT) specimens at stress intensities in the range 32 to 47 $\text{MPa}\cdot\text{m}^{1/2}$ for times as long as 52 weeks.^{11,13-14} Rebak reported that Alloy 22 U-bend specimens did not suffer SCC when exposed to 45% MgCl_2 at 154°C for up to 6 weeks.¹² Estil et al. performed SSRT at a $1.6 \times 10^{-6} \text{ s}^{-1}$ strain rate at the corrosion potential (E_{corr}) in saturated CaCl_2 (>10M Cl^-) at 120°C and 1% PbCl_2 at 95°C.¹⁶ None of these specimens showed a loss of ductility or secondary cracking.¹⁶

Even though Alloy 22 is resistant to SCC in concentrated chloride solutions, it may be susceptible under other severe environmental conditions.¹⁷⁻²¹ Andresen et al. tested the susceptibility of Alloy 22 to EAC at the corrosion potential (E_{corr}) in basic saturated water (BSW) at 110°C.¹⁷ This BSW multi-ionic solution is a version of concentrated solutions that might be obtained after evaporative tests of Yucca Mountain ground waters. Using the reversing DC potential drop technique, Andresen et al. reported a crack growth rate of $5 \times 10^{-13} \text{ m/s}$ in a 20% cold-worked specimen loaded to a stress intensity of 30 $\text{MPa}\cdot\text{m}^{1/2}$. This EAC testing was carried out in air saturated BSW water of pH ~13. The testing conditions used by Andresen et al. were highly aggressive and, in spite of that, the measured crack growth rate was near the detection limit of the system.¹⁷ Rebak et al. reported that Alloy 22 U-bend specimens suffered transgranular SCC when they were exposed for 336 h to aqueous solutions of 20% HF at 93°C and to its corresponding vapor phase.¹⁸ The liquid phase was more aggressive than the vapor phase.¹⁸ Pulvirenti et al. reported transgranular cracking in one out of four Alloy 22 U-bend specimens exposed for 15 days at 250°C in concentrated ground water contaminated with 0.5% lead (Pb) and acidified to pH 0.5.¹⁹⁻²⁰ Estil et al. performed slow strain rate tests, cyclic loading tests and U-bend tests in large variety of environments (temperature, applied potential and solution composition).²¹ They only reported SCC on MA Alloy 22 through SSRT in saturated concentrated water (SCW) at 73°C and at a potential of +0.4V [SSC].²¹

Recent published studies found that Alloy 22 was resistant to stress corrosion cracking (SCC) in hot concentrated chloride solutions and in simulated concentrated water (SCW) and other concentrated ground waters.²²⁻²⁴ Compact tension (CT) specimens of Alloy 22 were tested for over 3000 hours at an applied stress intensity of 47 $\text{MPa}\cdot\text{m}^{1/2}$ in 9.1M LiCl solution at 95°C. None of the specimens suffered SCC even at applied potentials higher than the crevice repassivation potential.²² A similar test was run on an Alloy 22 CT specimen at an applied potential of +380 mV [SCE] in SCW solution at 73°C and 95°C. The specimen was free from SCC.²² The same investigators reported that Alloy 22 U-bend specimens did not crack in presence of supersaturated PbCl_2 pH 0.5 at 95°C after more than 40 days of testing.²² It was also reported that welded and non-welded Alloy 22 U-bend specimens exposed in SCW at 90°C and at +400 mV SSC were free from EAC after 28 days. From References 22-23, it is apparent that Alloy 22 would suffer EAC in hot SCW at +400 mV SSC under continuous deformation or dynamic loading (SSRT) but would not suffer EAC under constant loading or constant deformation, at least during the testing time reported.²²⁻²³ Similarly to results reported in Reference 17 using a combination of cyclic and constant loading and monitoring crack growth in concentrated ground waters by the reversing DC potential drop technique, Andresen et al. continued their testing program on Alloy 22, adding 20% cold worked and thermally aged materials.²⁴ They reported some of the lowest ever measured crack propagation rates in the order of $2 \times 10^{-13} \text{ m/s}$ and described that it is exceedingly unlikely that Alloy 22 would suffer SCC under the container static emplacement conditions.

The effect of embrittlement by hydrogen entrance into the metal is commonly evaluated by applying mechanical deformation to specimens under cathodic applied potentials (or currents). Earlier studies on hydrogen

drogen damage of Ni-Cr-Mo alloys were performed using alloy C-276, mostly regarding oil and gas exploration studies.²⁵⁻²⁶ The first evidence of hydrogen damage of Alloy 22 was reported in 1991 using slow strain rate tests (SSRT) at a deformation rate of 4×10^{-6} in/s.²⁷ That is, SSRT tests were conducted on Alloy 22 electrodes pre-charged with hydrogen for 24 h by applying a cathodic current density of 20 mA/cm² and continuing during the straining tests in 0.1 M sodium sulfate (Na₂SO₄) solution at 20°C, 50°C and 85°C.²⁷ The baseline time to failure and reduction in area at rupture in inert test conditions (air) for Alloy 22 were 165 h and 75%, respectively. Under cathodic charging, the times to failures were 118 h, 135 h and 160 h and the reductions in area 43%, 48% and 64% both at 25°C, 50°C and 85°C, respectively.²⁷ That is, the higher the temperature, the lower the suffered embrittlement. For example, at 25°C, the time to failure was reduced 28% as compared to air, while at 85°C the reduction in the time to failure was only 3%. Abundant secondary cracking was reported for the specimen strained at 25°C.²⁷ This is a phenomenon attributed to hydrogen damages such as hydrogen embrittlement (HE) or hydrogen induced cracking (HIC).^{26,28} In another similar study, Alloy 22 electrodes were also cathodically pre-charged at 20 mA/cm² and then SSRT tested in 0.1 N H₂SO₄ solutions, presumably at the ambient temperature. The pre-charge treatments were carried for 1 and 2 weeks and charging continued throughout the straining.²⁹⁻³⁰ The used strain rate was not stated but the authors reported that an annealed Alloy 22 specimen strained presumably in air (no charging) ruptured after 182 h of straining. A specimen that was pre-charged for 1 week failed at 149 h of straining and a specimen charged for 2 weeks failed after 134 h of straining. Under the same conditions, the reduction in area varied from 80% (no charging), to 63% (1 week charging) to 55% (2 week charging).²⁹⁻³⁰ The authors also studied the effect of thermal aging (100 h at 500°C) and cold working on the susceptibility of Alloy 22 to cathodic charging and they found even stronger loss of ductility due to environmental effects than for the mill annealed material. They attributed this behavior to hydrogen damage.²⁹⁻³⁰

The purpose of the present work was to use SSRT to explore the influence of applied potential, temperature and electrolyte composition on the susceptibility of Alloy 22 to suffer EAC.

EXPERIMENTAL

The SSRT specimens were machined from wrought mill annealed plate stock (Heat 2277-8-3126). The chemical composition of the alloy in weight percent was: ~57% Ni, 21.7% Cr, 13.26% Mo, 2.8% W, 3.59% Fe, 1.03% Co, 0.27% Mn, 0.14% V, 0.004% C and 0.001% S. The typical mechanical properties of MA plate material are listed in Table 1. The specimens were tested in the as-machined condition, which corresponded to a root mean square (RMS) roughness of 32 μ-inch. The specimens were degreased in acetone before testing. Each specimen was cylindrical, approximately 7.25 -inch (184 mm) long and 0.438 -inch (11 mm) diameter. The useful gage of the specimens was 1 -inch (25.4 mm) long and had a 0.1 -inch (2.54 mm) diameter. Only the useful gage section was exposed to the electrolyte solution. Other areas of the specimens were covered with a protective coating. The slow strain rate tests were conducted at a constant deformation rate of 1.67×10^{-6} s⁻¹.

Tests were carried in simple solutions such as in sodium fluoride (NaF) (Table 2) and in simulated concentrated water (SCW), which is a complex electrolyte simulating an environment that would be obtained after reducing the volume of ground water from the Yucca Mountain site approximately 1000 times through evaporation. The used composition of SCW in mg/L was: 3,400 potassium (K), 40,900 sodium (Na), 1,400 fluorine (F), 6,700 chlorine (Cl), 6,400 nitrate (NO₃⁻), 16,700 sulfate (SO₄²⁻), 70,000 bicarbonate (HCO₃⁻) and approximately 40 silicon (SiO₂). The most likely environments at the emplacement site at Yucca Mountain would contain a wide variety of ions as a consequence of interactions

between water and minerals in the mountain. ³¹⁻³³ The electrolyte solutions were naturally aerated; that is, a stream of air was circulated above the level of the electrolyte solution. All tests were carried out under ambient pressure. Some tests were carried at the free corroding potential (E_{corr}) and others were carried under applied potential. The corrosion potentials (E_{corr}) before each test are reported in Table 2. During the straining tests, the current was continuously recorded for the polarized electrodes and the free corrosion potential was recorded for the non-polarized electrodes. The electrochemical potentials in this paper are reported in the saturated silver-silver chloride scale [SSC]. At ambient temperature, the SSC scale is 199 mV more positive than the normal hydrogen electrode (NHE). After testing, the samples were evaluated using optical and scanning electron microscopy (SEM).

The slow strain rate technique (SSRT) is an efficient tool to assess the susceptibility of a metal (alloy) to suffer environmentally assisted cracking (EAC) such as stress corrosion cracking (SCC) and hydrogen induced cracking (HIC). This technique is described by the ASTM standard G129, and is not intended to represent service performance. ³⁴ SSRT is an accelerated screening method to examine, for example, the influence of environmental and metallurgical variables on EAC. During SSRT tests, the specimen is slowly deformed by constant elongation rate (CER) until it ruptures. The deformation rate used in the tests reported here was 0.0001002 inch per minute or approximately $1.67 \times 10^{-6} \text{ sec}^{-1}$. At this deformation rate, a one-inch (25.4 mm) long gage of the ductile Alloy 22 could take up to 5–6 days to break. The susceptibility to EAC can then be measured by the time to failure of the specimen or the maximum load reached during straining as compared to a specimen tested in inert conditions (air). The lower the time to failure, the more likely the test conditions would cause EAC in the alloy of interest. Similar analysis can be made for the maximum load. Otherwise, the susceptibility to EAC could also be assessed by measuring the reduction of area (RA) of the specimen at the moment of rupture. A ductile specimen offers high reduction of area (necking) while a specimen that is suffering EAC may offer a low reduction of area.

RESULTS AND DISCUSSION

Effect of the Applied Potential

Table 2 shows experimental results from the SSRT tests. A few of the results listed in Table 2 were published before. ²¹ Table 2 details the corrosion potential (E_{corr}) of the specimen before the potential of interest was applied, the applied potential during the tests, the time to failure during constant deformation rate straining, the maximum stress (load) attained during straining and the reduction of area (RA) of the specimen (necking) at the moment of rupture.

The effect of applied potential was studied mainly in the SCW solution both hot (73–90°C) and at ambient temperature (~22°C). Figure 1 shows the stress-strain curves for specimens tested at three different applied potentials. The higher the applied potential, the lower the strain (time) to rupture. Figure 2 summarizes the time to failure of Alloy 22 in hot and ambient SCW as a function of the applied potential. In hot (73–86°C) SCW, the longest time to failure or lowest susceptibility to EAC corresponded to the specimen strained at the free corrosion potential (E_{corr}) or at approximately –150 mV SSC. The time to failure decreased as the applied potential shifted in either the anodic or cathodic direction (Figure 2). As the applied potential increased in the anodic direction up to +400 mV SSC, the time to failure decreased rapidly from near 125 h to approximately 80 h (Table 2 and Figure 2). In the cathodic side of potentials, the decrease was less pronounced. In SCW at 90°C and –1000 mV SSC, the time to failure decreased only to near 110 h. On the other hand, in the SCW solution at ambient temperature, the behavior of strained Alloy 22 was almost the opposite that the one in the hot SCW solution. That is, at the c

thodic potential of -1000 mV SSC the time to failure was 100 h (Table 2 and Figure 2) and in the anodic direction practically there was no reduction of the time to failure (Figure 2). That is, the susceptibility to EAC in hot SCW increased as the anodic potential increased but in ambient SCW, the susceptibility to EAC increased in the cathodic region of potentials.

Figure 3 shows the appearance of the strained Alloy 22 electrodes in hot SCW solution, both at the corrosion potential (E_{corr}) and at the anodic potential of $+400\text{ mV SSC}$. The mode of failure at E_{corr} was ductile with a reduction of area of 80% (Table 2) and without secondary cracking (Figure 3). At $+400\text{ mV SSC}$, the specimen failed with little reduction of area (44%) and had a high concentration of typical EAC secondary cracking (Figure 3). Figure 4 shows the appearance of the electrodes strained at -1000 mV SSC both at 90°C and at ambient temperature. The EAC effect was more pronounced at ambient temperature. Figure 3(c) and Figure 4(a and c) show the difference in the fracture mechanism between anodic and cathodic potentials. Macroscopically, at anodic potential (Fig. 3c) the fracture was almost perpendicular to the straining direction; however, at cathodic potential (Fig. 4a and c) the fracture plane was oriented approximately at 45° from the straining direction. In a more microscopic scale, the secondary cracks are almost indistinguishable (Figures 3 and 4, d); however, it appears to be more grain boundary localized at the cathodic than at the anodic potentials. Figure 4a and c show little reduction in area in both specimens strained at -1000 mV SSC , of similar magnitude than the specimen strained in hot SCW at $+400\text{ mV SSC}$ (Figure 3c). Table 2 shows that the RA for specimens ARC22-031 and 036 were respectively 48% and 43% and for specimen ARC22-033 was 44%. However, Figure 4c shows a much lower amount and depth of secondary cracking than Figure 3c. It is evident that a different cracking mechanism was operating at cathodic potential than at anodic potential. When Alloy 22 specimens were strained to rupture in air, the fracture region has pronounced necking or reduction in area (Table 2) similar to the observed at E_{corr} (Figure 3a).

One Alloy 22 specimen (ARC22-094 in Table 2), which was thermally aged by exposure to 700°C for 173 h, was strained in SCW at 86°C at a potential near E_{corr} . Even though this specimen contained second phase precipitates as a consequence of the thermal aging, it exhibited little effect of EAC similar to the mill annealed (non-aged) specimen tested in similar conditions.

Effect of the Temperature

Temperature seems to play an important role on the susceptibility of Alloy 22 to EAC. Figure 5 shows the stress-strain curves for two specimens strained at the same applied potential ($+400\text{ mV}$) but at different temperatures. The specimen strained at ambient temperature had an elongation to rupture similar to the one in air, however the specimen strained at 73°C had an elongation to rupture approximately 25% lower. Figure 6 shows that, as the temperature increased, the time to failure for the specimens strained in SCW at $+400\text{ mV SSC}$ decreased. The decrease in the time to failure as the temperature increased seemed practically continuous, without an apparent threshold value. However, Figure 7 shows that there is an obvious difference on the appearance of the strained electrodes after rupture. The specimen strained at 65°C had considerably more evidence of EAC than the specimen strained at 50°C (Figure 7).

The effect of the temperature on the susceptibility of Alloy 22 to EAC was also evident in the cathodic region of potentials. However, in the cathodic region, the effect of the temperature was just the opposite as in the anodic region of potentials. That is, the susceptibility of Alloy 22 to EAC in SCW solution was more pronounced at ambient temperature than at 90°C . Similar findings were reported before by other researchers.^{27,29-30} Figure 4(a and c) shows the characteristics of two electrodes, one strained at 90°C

(Fig.4a) and the other at ambient temperature (Fig.4c). It is apparent that the specimen strained at ambient temperatures suffered a higher amount of secondary cracking.

Effect of the Electrolyte Composition

The main focus of the research reported here was to evaluate the response of Alloy 22 electrodes strained in SCW solution at different temperatures and applied potentials. It was reported before that Alloy 22 was susceptible to EAC in SCW solution but it did not suffer cracking in other versions of concentrated ground waters such as SAW and BSW.¹⁶⁻²¹ A few tests were carried out to try to identify the components of SCW that could be responsible for the EAC of Alloy 22. Table 2 shows the results of straining tests performed in NaF and NaCl solutions. Figure 8 shows the stress-strain curves of Alloy 22 at anodic applied potentials in three different environments. Even though the applied potentials and temperatures are not exactly the same between test and test shown in Figure 8, it is apparent that SCW was more aggressive than 1 M NaF solution and NaF more aggressive than the NaCl solution. Table 2 and Figure 2 also shows that at the cathodic applied potential, the time to failure was longer in the NaF solution than in the SCW solution.

Figure 9 shows the appearance of the electrodes strained in NaF and NaCl solutions. Figures 9a and b show that NaF solution produced shallow brittle transgranular secondary cracks on the surface of the strained electrode; however, the NaCl solution did not cause any EAC damage to the electrode (Figure 9c). It is apparent that fluoride ions, as one of the components of SCW, could be partially responsible for the embrittlement at the anodic potentials in SCW (Figures 2 and 3); however, under the same tested conditions, the SCW solution was far more aggressive than the pure fluoride solution (Figures 2 and 8). It is likely that more than one component in SCW could act synergistically to produce the damage observed in the hot SCW solution at the anodic potentials. This needs to be studied further, probably by preparing partial SCW solutions; that is, removing one constituent at the time and observing the effect on the EAC of Alloy 22.

CONCLUDING REMARKS

Results from testing show that Alloy 22 is practically immune to EAC in concentrated chloride solutions both at the corrosion potential and at anodic potentials. Alloy 22 may suffer SCC in hot SCW solution in the anodic potential and small amount of hydrogen damage in ambient SCW at the highly cathodic potential of -1000 mV SSC. In the vicinity of the corrosion potential, Alloy 22 was free of any EAC. Moreover, it has been shown that only actively loaded specimens (e.g. SSRT) would crack in hot SCW at anodic applied potentials.²²⁻²³ That is, specimens containing residual stresses or constant load and subjected to anodic polarization in hot SCW would not suffer EAC. Nevertheless, for conservative purposes, before emplacement, it is planned to relieve the welding induced residual stresses of the containers by either laser peening or burnishing.³

CONCLUSIONS

- (1) Millannealed (MA) Alloy 22 was susceptible to EAC in hot SCW solution at anodic applied potentials approximately 300 - 400 mV more positive than E_{corr} .
- (2) In the anodic region of potentials, the susceptibility to EAC decreased as the temperature decreased. EAC was not observed for specimens strained in SCW at ambient temperature.
- (3) Alloy 22 also suffered EAC in SCW at -1000 mV SSC, especially at ambient temperature.
- (4) Fluoride seems more detrimental than chloride for the EAC resistance of Alloy 22.

ACKNOWLEDGMENTS

This work was performed under the auspices of the U.S. Department of Energy (DOE) by the University of California Lawrence Livermore National Laboratory under contract N° W-7405-Eng-48. This work is supported by the Yucca Mountain Project, LLNL, which is part of the Office of Civilian Radioactive Waste Management (OCRWM), DOE.

REFERENCES

1. Yucca Mountain Science and Engineering Report, U.S. Department of Energy, Office of Civilian Radioactive Waste Management, DOE/RW-0539, Las Vegas, NV, May 2001.
2. G. A. Cragolino, D. S. Dunn and Y. -M. Pan in Scientific Basis for Nuclear Waste Management XXV, Vol. 713, pp. 53 - 60 (Warrendale, PA: Materials Research Society 2002).
3. G. M. Gordon, Corrosion, 58, 811 (2002).
4. Annual Book of ASTM Standards, Nonferrous Metal Products, Vol 02.04, B574 and B575 (West Conshohocken, PA: ASTM International, 2002).
5. P. E. Manning, J. D. Schöbel, Werkstoffe und Korrosion, 37, 137 - 145 (1986).
6. HASTELLOY C-22 Alloy, Publication H-2019E (Kokomo, IN: Haynes International Inc., 1997).
7. K. A. Gruss, G. A. Cragolino, D. S. Dunn, N. Sridhar, Paper 149, Corrosion/98 (Houston, TX: NACE International 1998).
8. R. B. Rebak in Corrosion and Environmental Degradation, Volume II, pp. 69 - 111 (Weinheim, Germany: Wiley - VCH 2000).
9. R. B. Rebak and P. Crook, Advanced Materials and Processes, 157(2), 37 (2000).
10. J. H. Lee, K. G. Mon, D. E. Longsine, B. E. Bullard and A. M. Monib in Scientific Basis for Nuclear Waste Management XXV, Vol. 713, pp. 61 - 70 (Warrendale, PA: Materials Research Society 2002).

11. Y.-M. Pan, D. S. Dunn and G. A. Cragnolino in *Environmentally Assisted Cracking: Predictive Methods for Risk Assessment and Evaluation of Materials, Equipment and Structures*, STP 1401, pp. 273- 288 (West Conshohocken, PA: ASTM 2000).
12. R. B. Rebak in *Environmentally Assisted Cracking: Predictive Methods for Risk Assessment and Evaluation of Materials, Equipment and Structures*, STP 1401, pp. 289 -300 (West Conshohocken, PA: ASTM 2000).
13. D. S. Dunn, G. A. Cragnolino and N. Sridhar in *Scientific Basis for Nuclear Waste Management XXIII*, Vol. 608, pp. 89 -94 (Warrendale, PA: Materials Research Society 2000).
14. D. S. Dunn and C. S. Brosia, Paper 125, *Corrosion/01* (Houston, TX: NACE International 2001).
15. D. S. Dunn, Y. -M. Pan and G. A. Cragnolino, Paper 425, *Corrosion/02* (Houston, TX: NACE International 2002).
16. J. C. Estill, K. J. King, D. V. Fix, D. G. Spurlock, G. A. Hust, S. R. Gordon, R. D. McCright, G. M. Gordon and R. B. Rebak, Paper 535, *Corrosion/02* (Houston, TX: NACE International 2002).
17. P. L. Andresen, P. W. Emigh, L. M. Young and G. M. Gordon, Paper 130, *Corrosion/01* (Houston, TX: NACE International 2001).
18. R. B. Rebak, J. R. Dillman, P. Crook and C. V. V. Shawber, *Materials and Corrosion*, 52, pp. 289-297 (2001).
19. A. L. Pulvirenti, K. M. Needham, M. A. Adel -Hadadi, C. R. Marks, J. A. Gorman and A. Barkatt in *Scientific Basis for Nuclear Waste Management XXV*, Vol. 713, pp. 89 -95 (Warrendale, PA: Materials Research Society 2002).
20. A. L. Pulvirenti, K. M. Needham, M. A. Adel -Hadadi, A. Barkatt, C. R. Marks and J. A. Gorman, Paper 551, *Corrosion/02* (Houston, TX: NACE International 2002).
21. K. J. King, J. C. Estill and R. B. Rebak, 2002 PVP -Vol. 449, pp. 103 -109 (New York, NY: American Society of Mechanical Engineers 2002).
22. G. A. Cragnolino, D. S. Dunn and Y. -M. Pan, Paper 03541, *Corrosion/03* (Houston, TX: NACE International 2003).
23. D. V. Fix, J. C. Estill, G. A. Hust, K. J. King, S. D. Day and R. B. Rebak, Paper 03542, *Corrosion/03* (Houston, TX: NACE International 2003).
24. P. L. Andresen, P. W. Emigh, L. M. Young and G. M. Gordon, Paper 03683, *Corrosion/03* (Houston, TX: NACE International 2003).
25. N. Sridhar, J. A. Kargol and N. F. Fiore, *Scr. Metall.*, 14, 225 (1980).
26. N. Sridhar and G. Cragnolino "Stress -Corrosion Cracking of Nickel -Base Alloys" in *Stress - Corrosion Cracking, Materials Performance and Evaluation*, p. 131 (Materials Park, OH: ASM International, 1992).
27. S. Kesavan, Ph.D. Dissertation, The Ohio State University (1991).
28. N. Sridhar, G. A. Cragnolino and D. S. Dunn, *Experimental Investigations of Failure Processes of High -Level Radioactive Waste Container Materials*, CNWRA 95 -010 (San Antonio, TX: Center for Nuclear Waste Regulatory Analyses, 1995).
29. K. M. Scammon, M.S. Thesis, University of Central Florida (1994).
30. V. H. Desai and K. M. Scammon, *Corrosion/95*, Paper 95161 (Houston, TX: NACE International 1995).
31. N. D. Rosenberg, G. E. Gdowski and K. G. Knauss, *Applied Geochemistry*, 16 (2001), pp. 1231 -1240.
32. G. E. Gdowski, T. J. Wolery and N. D. Rosenberg in *Scientific Basis for Nuclear Waste Management XXV*, Vol. 713, pp. 29 -36 (Warrendale, PA: Materials Research Society 2002).
33. R. T. Pabalan, L. Yang and L. Browning in *Scientific Basis for Nuclear Waste Management XXV*, Vol. 713, pp. 37 -44 (Warrendale, PA: Materials Research Society 2002).

34. Annual Book of ASTM Standards, Wear and Erosion; Metal Corrosion, Vol 03.02, G129 (West Conshohocken, PA: ASTM International, 2003).

TABLE 1
TYPICAL MECHANICAL PROPERTIES OF PLATE AND SHEET ALLOY 22

Heat	Tensile Strength [UTS] (MPa)	Yield Stress [0.2%] (MPa)	Elongation to Rupture (%)	Hardness (RB)	ASTM Grain Size
Sheet – 2277 -8- 3203	824	412	62	92	5.5
Plate – 2277 -8-3126	766	387	64.4	83	4

TABLE2
SLOWSTRAINRATE($\sim 1.67 \times 10^{-6} \text{S}^{-1}$)TESTINGOFMAALLO Y22

Sample	Solution	pH	Temp. (°C)	E_{corr} (mV, SSC)	$E_{\text{app.}}$ (mV, SSC)	Time to Failure (h)	UTS (MPa)	RA (%)	Observations Stereomicroscope X40 and X100
012	Air	None	22 ^(A)	None	None	124	786	74	Ductile, Necking
040	Air	None	22	None	None	123	813	70	Ductile, Necking
031	SCW	9-10	90	-168	-1000	111	746	48	Shallow incipient SCC. Little or no necking
034	SCW	9-10	90	-143	E_{corr}	129	712	80	No SCC. Necking
094 (B)	SCW	9-10	86	-123	-23	116	751	66	Dark Sample. Shallow incipient SCC. No necking
026	SCW	9-10	73	-241	+100	120	764	79	Ductile Failure, necking. No SCC
023	SCW	9-10	73	-224	+200	DNB	DNB	72	Necking. Incipient or Shallow SCC
025	SCW	9-10	73	-172	+200	116	776	80	Necking. Incipient or Shallow SCC
029	SCW	9-10	89	-144	+200	112	678	73	Necking. Incipient or Shallow SCC
030	SCW	9-10	85	-182	+300	98	725	65	SCC
113	SCW	9-10	75	-200	+317	116	765	63	Shallow incipient SCC. Dissolution
032	SCW	9-10	50	-129	+400	110	757	75	Shallow incipient SCC. Necking
134	SCW	9-10	65	-217	+400	97	684	59	SCC
021	SCW	9-10	73	-172	+400	90	665	64	SCC
112	SCW	9-10	73	-93	+400	91	697	71	SCC
033	SCW	9-10	86	-169	+400	76	642	44	SCC
036	SCW	9-10	22	-43	-1000	100	785	43	Incipient SCC. No necking
132	SCW	9-10	22	-97	-750	118	792	70	Shallow incipient SCC
038	SCW	9-10	22	-66	-500	117	798	82	Necking. No SCC
037	SCW	9-10	22	-76	E_{corr}	DNB (C)	DNB	32	No SCC
020	SCW	9-10	22	-109	+291	116	800	85	Ductile Failure, necking. No SCC
133	SCW	9-10	22	-128	+400	124	798	80	Necking. No SCC
123	4MNaCl	6.2	98	-323	+349	127	762	80	No SCC. Necking
098	1MNaCl	6.9	90	-104	+400	74 (D)	660	76	No SCC. Crevice Corrosion
099	1MNaF	10	22	-159	-1000	115	794	65	Shallow incipient SCC. Necking
091	1MNaF	9.2	85	133	E_{corr}	112	756	67	No SCC. Necking
130	1MNaF	7.6	90	-244	+400	112	727	67	Incipient SCC. Necking.

(A) Tested at Ambient Temperature, (B) Sample aged at 700°C for 173h. (C) DNB = Did not break (equipment stoppage), (D) Short failure time due to crevice corrosion at the coating interface.

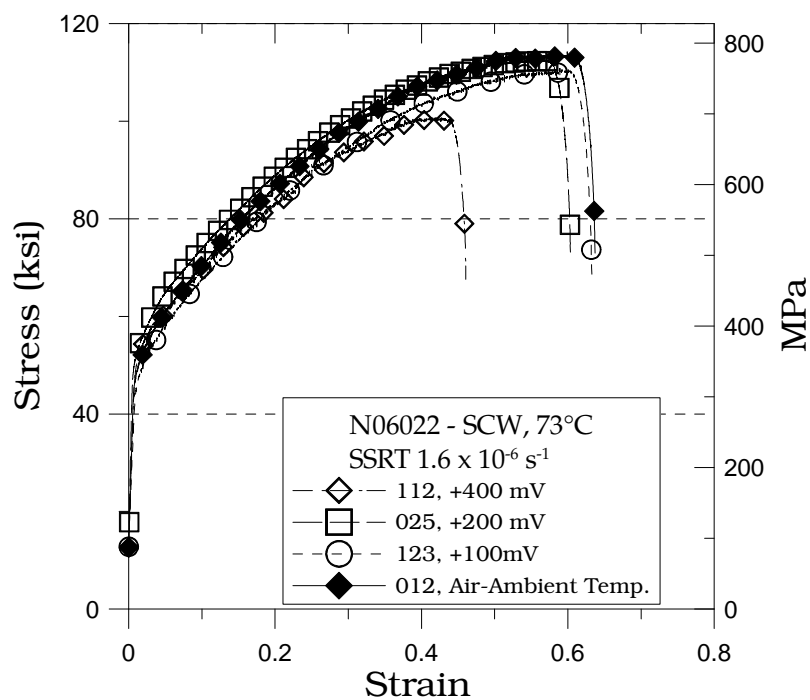


FIGURE1: Stress -Strain curves of Alloy 22 in SCW as a function of the applied potential.

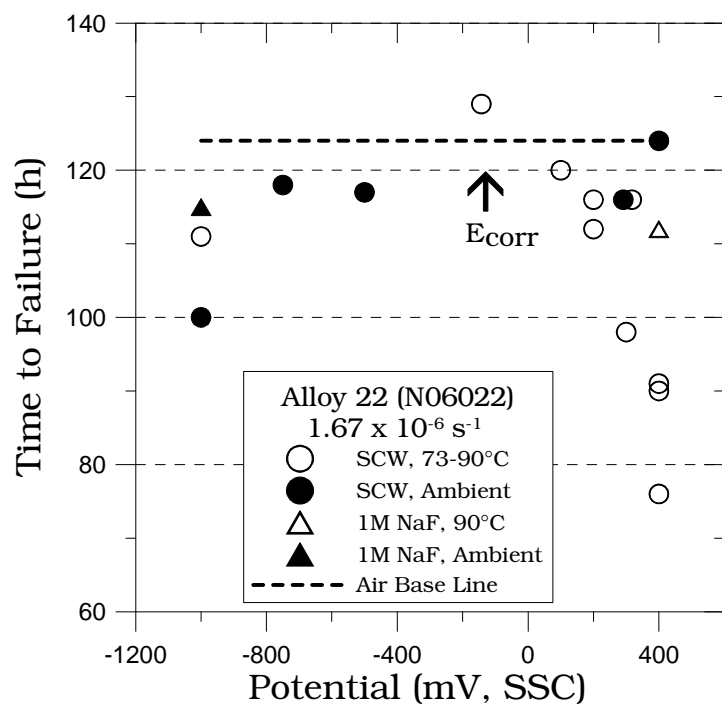
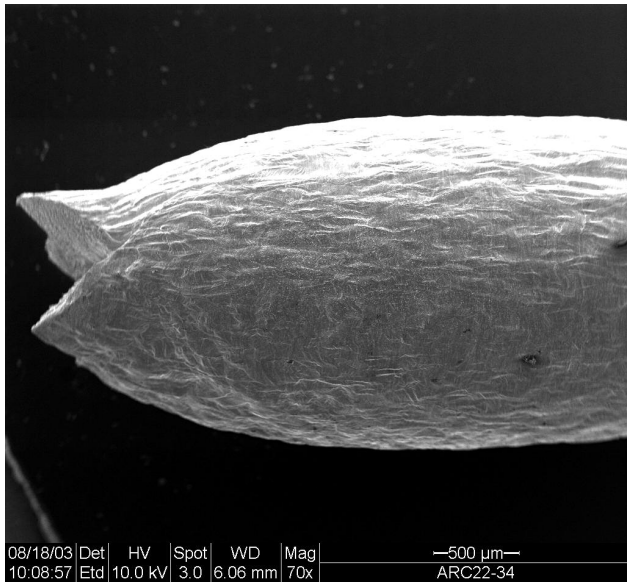
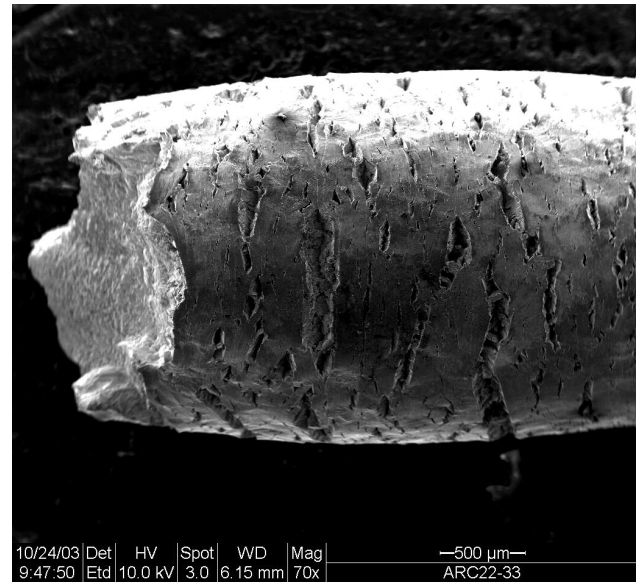


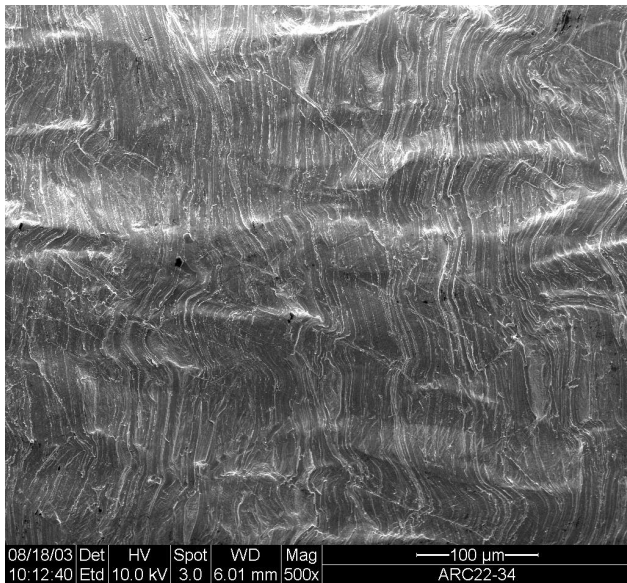
FIGURE2: Time to failure of Alloy 22 specimens strained at different potentials.



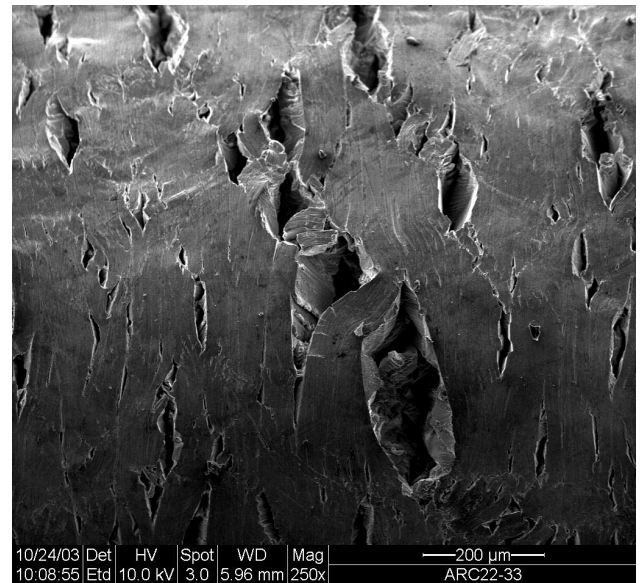
(a) MagnificationX70



(c) MagnificationX70



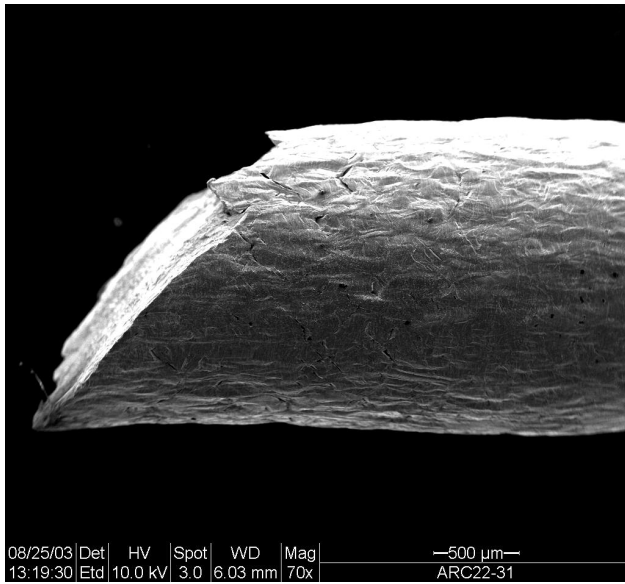
(b) MagnificationX500



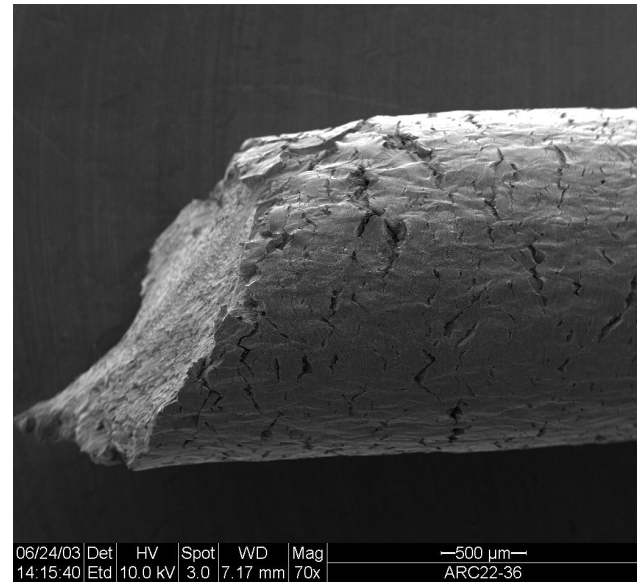
(d) MagnificationX250

FIGURE3: SEM images of Alloy 22 specimens strained in SCW: (a) and (b) ARC22
(c) and (d) ARC -033, 86°C, +400mV SSC).

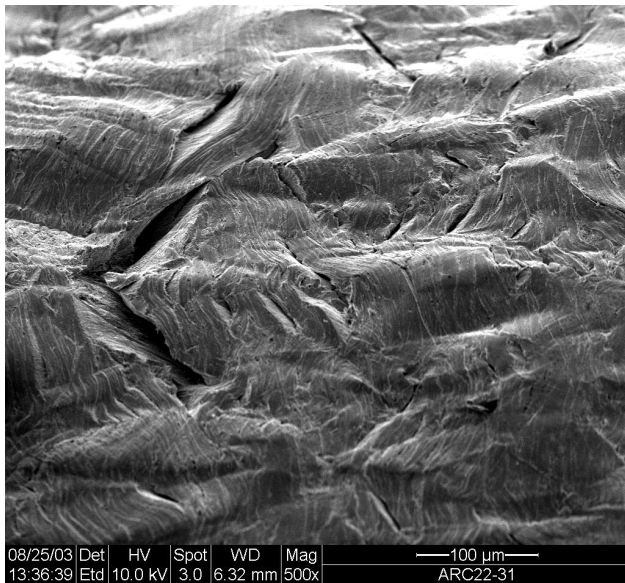
-034, 90°C, E_{corr}



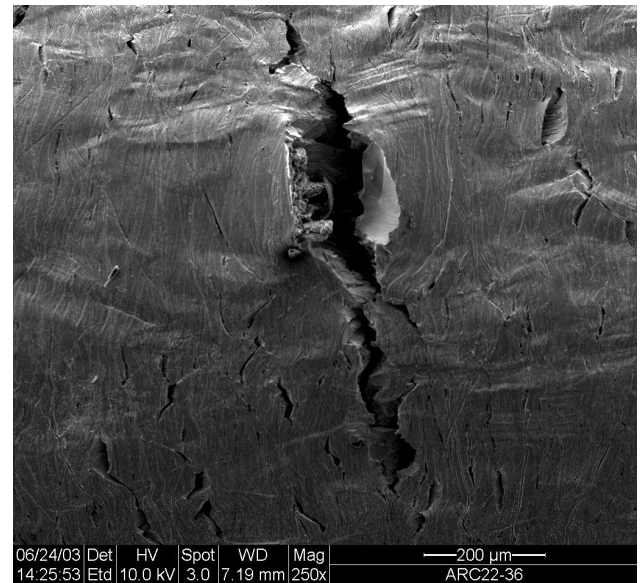
(a) MagnificationX70



(c) MagnificationX70



(b) MagnificationX500



(d) MagnificationX250

FIGURE4:SEMimagesofAlloy22specimensstrainedinSCW:(a)and(b)ARC22 -031,90°C, -1000 mVSSC(c)and(d)ARC -036,22°C, -1000mVSSC).

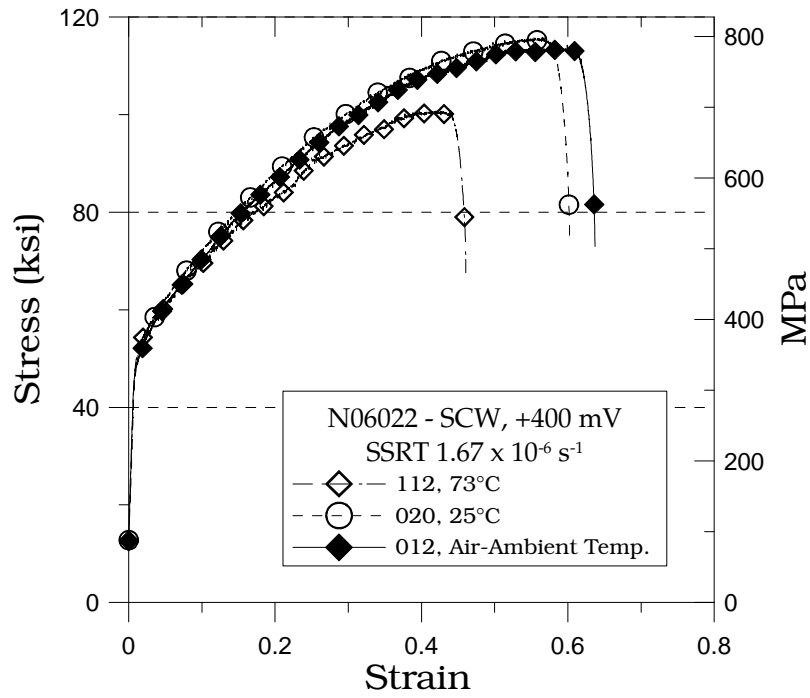


FIGURE5: Stress -Strain curves of Alloy 22 in SCW as a function of the temperature.

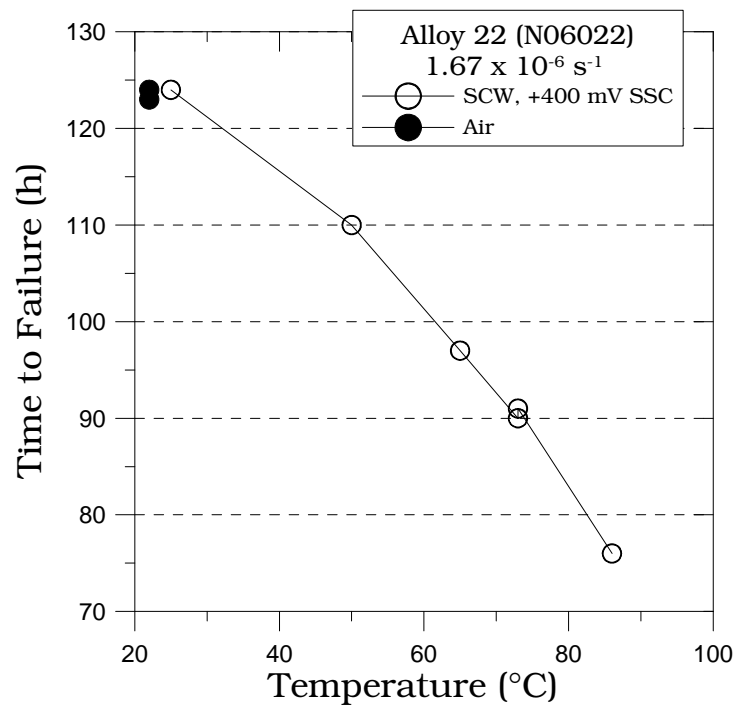
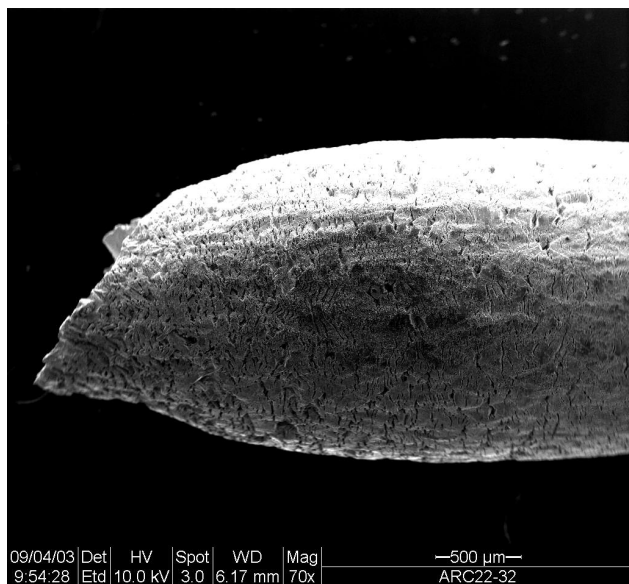
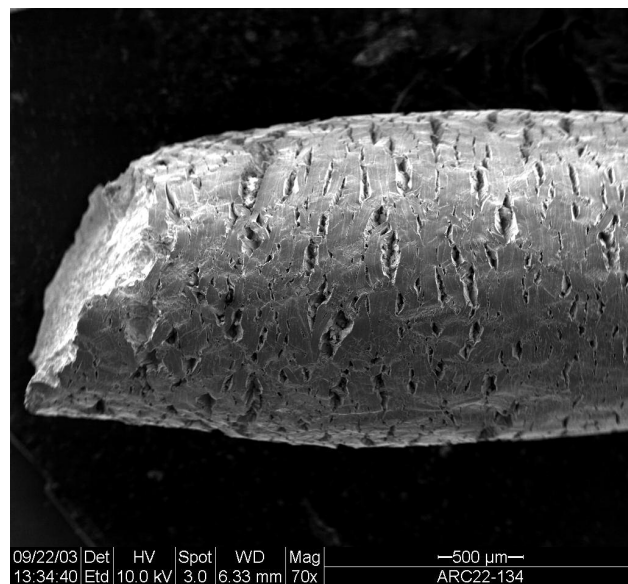


FIGURE6: Time to failure of Alloy 22 specimens strained at different temperatures.



(a) Magnification X70



(b) Magnification X70

FIGURE7: SEM images of Alloy 22 specimens strained in SCW at +400 mV SSC: (a) ARC22 -032 at 50°C and (b) ARC -134 at 65°C.

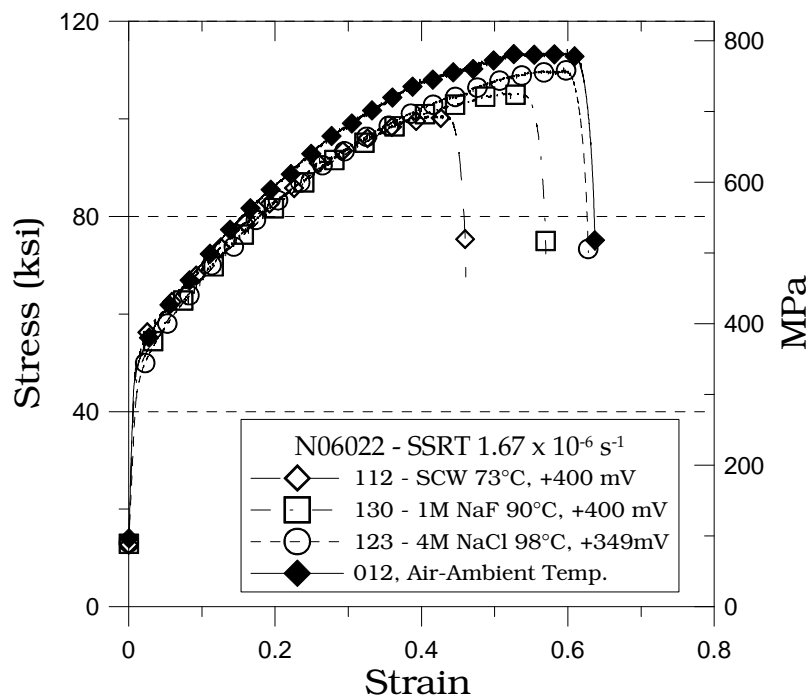
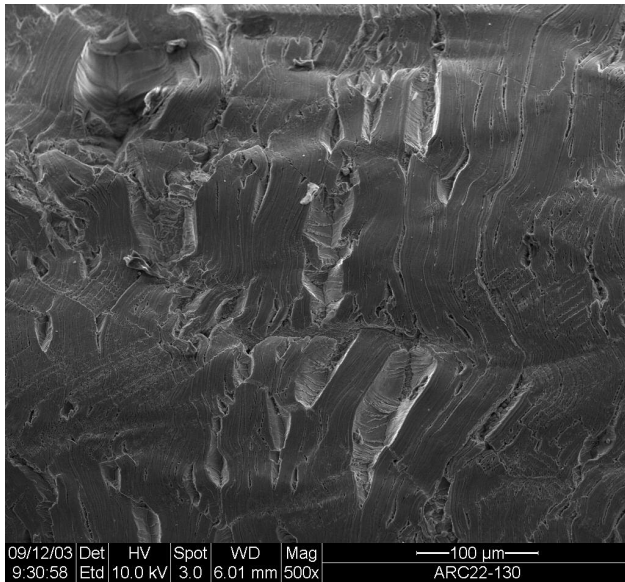
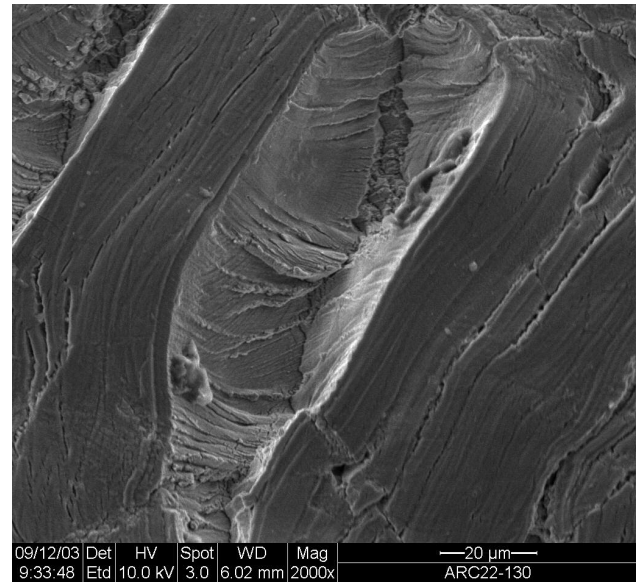


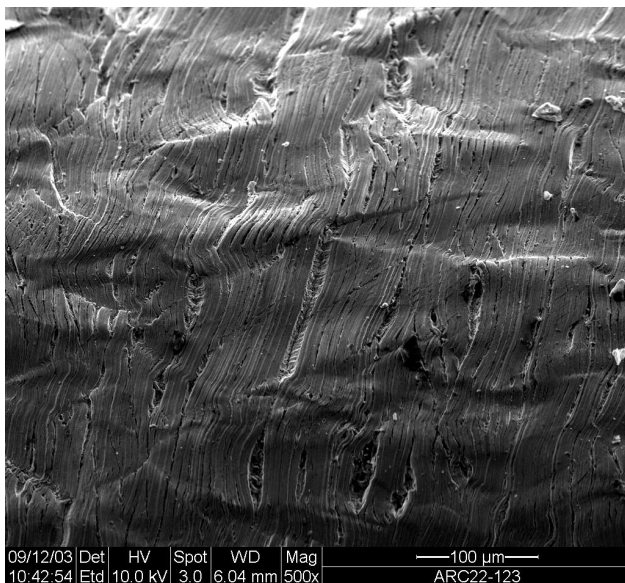
FIGURE8: Stress -Strain curves of Alloy 22 in SCW as a function of the electrolyte composition.



(a) MagnificationX500



(b) MagnificationX500



(d) MagnificationX500

FIGURE9:SEMimagesofAlloy22specimensstrainedin:(a)and(b)ARC22 -130in1MNaFat90°C and+400mVSSCand(c)ARC -123in4MNaClat98°Cand+349mVSSC.